Transport in Porous Media (2006) 64: 413–422
DOI 10.1007/s11242-005-5479-7

On the Effect of Anisotropy on the Stability of Convection in Rotating Porous Media

SANESHAN GOVENDER*
School of Mechanical Engineering, University of Kwa-Zulu Natal, King George V Avenue, Durban 4041, South Africa

(Received: 1 September 2005; accepted in final form: 25 November 2005)

Abstract. We investigate natural convection in an anisotropic porous layer subjected to centrifugal body forces. The Darcy model (including centrifugal and permeability anisotropy effects) is used to describe the flow and a modified energy equation (including the effects of thermal anisotropy) is used in the current analysis. The linear stability theory is used to evaluate the critical Rayleigh number for the onset of convection in the presence of thermal and mechanical anisotropy. It is found that the convection is stabilized when the thermal anisotropy ratio (which is a function of the thermal and mechanical anisotropy parameters) is increased in magnitude.

Key words: mechanical anisotropy, thermal anisotropy, rotation, centrifugal Rayleigh number.

Nomenclature

Latin Symbols

g^*	acceleration due to gravity
H^*	height of the mushy layer
$\hat{\boldsymbol{e}}_z$	unit vector in the z-direction
k_x, k_y, k_z	characteristic permeabilities in the x-, y- and z- directions
L	length of the mushy layer
p	reduced pressure
R	rescaled Rayleigh number, Ra_ω/π^2
Ra_ω	Centrifugal Rayleigh number, $\beta_* \Delta T k_{*x} \omega_*^2 L_*^2 / (\kappa_{*x} \nu_*)$
s_y	y-component of wavenumber
s_z	z-component of wavenumber
t	time
T	dimensionless temperature, $(T^* - T_C)/(T_H - T_C)$
u	horizontal x-component of the filtration velocity
v	horizontal y-component of filtration velocity
w	vertical component of filtration velocity
$\boldsymbol{V}$	dimensionless filtration velocity vector, $u\hat{e}_x + v\hat{e}_y + w\hat{e}_z$

*e-mail: govenders65@nu.ac.za

$\boldsymbol{X}$	space vector, $x\hat{e}_x + y\hat{e}_y + z\hat{e}_z$
x	horizontal length co-ordinate
y	horizontal width co-ordinate
z	vertical co-ordinate

Greek Symbols

α	scaled wavenumber, s^2/π^2
β	thermal expansion coefficient
κ	fluid thermal diffusivity
μ	fluid dynamic viscosity
ν	fluid kinematic viscosity
ρ	fluid density
ω	angular velocity

Subscripts

$*$	dimensional quantities
o	scaled parameters
B	basic flow quantities
C	associated with cold wall
cr	critical values

1. Introduction

Over the past years, interest in fundamental studies of thermal convection in porous media has significantly increased due to its presence in diverse engineering applications in fields such as thermal insulation technology, pebble bed nuclear reactors, cooling of electronic equipment and binary alloy solidification. In general buoyancy induced flows in porous media plays an important role in engineering applications.

One important engineering application includes high speed centrifuge processes where the gravitational acceleration is small compared to the centrifugal acceleration. To choose another engineering application, let us consider binary alloy solidification as an example. In the solidification of binary alloys one finds the presence of three distinct layers viz. the solid layer, the melt layer and the mushy layer, which is sandwiched between the solid and melt regions. The mushy layer may be thought of as a two-phase zone/reactive porous medium that serves to smear the concentration gradient between the solid and melt regions. Experimental studies by Sample and Hellawell (1984) and Sarazin and Hellawell (1998) reveal important information on mechanism for channel formation. It is also demonstrated that the dynamics occurring in the mushy layer are critical to the quality of the final product. Amberg and Homsy (1993), Anderson and Worster (1995) and Worster (1992) provide an excellent numerical analysis of the effects of gravity on solidification, whilst Govender and Vadasz (2002) and Govender (2003) extend their work by proposing rotation as a means of stabilising convection. In all of the above studies dealing with the stability analysis in the mushy layer, investigators assumed isotropic permeability and thermal diffusivity in the mushy layer in order to simplify the analysis. In many engineering applications (including the mushy layer) the porous matrix is anisotropic both mechanically and thermally. A good review of convection in anisotropic porous media is provided by McKibbin (1986) and Storesletten (1993). Limited work dealing with anisotropy effects in porous media including rotational effects has been undertaken by Alex and Patil (2000), Patil *et al.* (1989) and Vaidyanathan *et al.* (1988). These works, however, are distinctly different from the current work in terms of geometry orientation and boundary conditions.

In the current study we extended the work of Vadasz (1994) to include both thermal and permeability anisotropy, with a view to application in binary alloy solidification. The effects of thermal and mechanical anisotropy on the convection threshold point (critical Rayleigh number) will be discussed.

2. Problem Formulation

Figure 1 shows a fluid saturated anisotropic porous layer of height L_* which is heated (T_{H}), at $x_* = 0$ and cooled (T_{C}) at $x_* = L_*$. In addition the porous layer is insulated vertically (i.e. $\partial T_* / \partial z_* = 0$) at $z_* = 0$ and $z_* = L_*$. The solid and fluid phases are in local thermodynamic equilibrium but

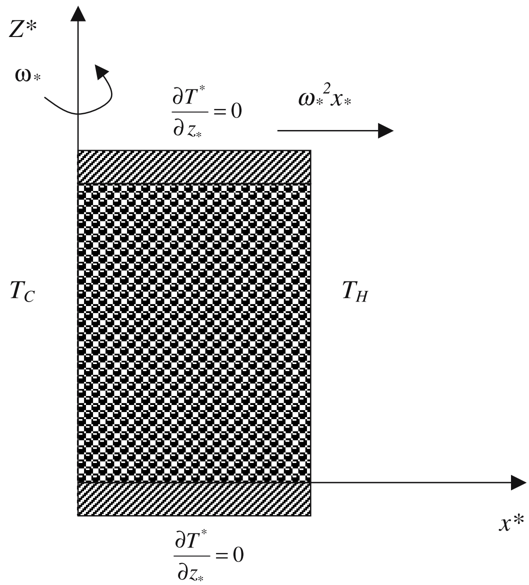

Figure 1. Porous layer subjected to centrifugal body forces and differential heating.

anisotropy exists both in permeability and thermal diffusivity. The dimensional governing equations are presented as follows for continuity, Darcy, and Energy:

$$\nabla_* \cdot \boldsymbol{V}_* = 0, \tag{1}$$

$$\boldsymbol{V}_* = \frac{K_*}{\mu_*}\left[-\nabla_* p_* + \rho_* g_* \hat{e}_g + \rho_* \omega_*^2 x_* \hat{e}_\omega\right], \tag{2}$$

$$\frac{\partial T_*}{\partial t_*} + V_* \cdot \nabla_* T_* = \nabla_* \cdot (\kappa_* \cdot \nabla_* T_*), \tag{3}$$

The symbols $\boldsymbol{V}_*$, T_* and p_* represent the dimensionless filtration velocity vector, temperature (subscript f for fluid phase and s for solid phase) and reduced pressure, respectively, and $\hat{e}_g$ and $\hat{e}_\omega$ are unit vectors in the direction of the gravity vector and rotation. The permeability and thermal conductivity tensors K_*, κ_* are defined as

$$K_* = k_{*x}\begin{bmatrix} 1 & 0 & 0 \\ 0 & \xi & 0 \\ 0 & 0 & \xi \end{bmatrix}, \quad \kappa_* = \kappa_{*x}\begin{bmatrix} 1 & 0 & 0 \\ 0 & \eta & 0 \\ 0 & 0 & \eta \end{bmatrix}, \tag{4}$$

and vertical thermal and mechanical isotropy has been assumed. In Equation (4) k_{*x} is the permeability in the x-direction and $\xi = k_{*y}/k_{*x} = k_{*z}/k_{*x}$, and κ_{*x} is the fluid thermal conductivity in the x-direction and $\eta = \kappa_{*y}/\kappa_{*x} = \kappa_{*z}/\kappa_{*x}$. The properties, μ_* and κ_* in Equations (1–3), refers to the fluid dynamic viscosity and thermal diffusivity. We may now non-dimensionalize the governing Equations (1–3) using the scaling variables H_*, κ_{*x}/H_*, $\kappa_{*x}\mu_*/k_{*x}$ and $H_*^2/\kappa_{*x}$to non-dimensionalize the length, velocity, pressure and time. The fluid and solid phase temperatures are scaled according to the relations, $T = (T_* - T_C)/\Delta T$ where $\Delta T = T_H - T_C$. To account for density variations (as a function of temperature), we adopt the Boussinesq approximation $\rho_* = \rho_{*0}[1 - \beta_*(T - T_C)]$. Applying the above scaling variables to Equations (1–3) and eliminating the pressure term from the momentum equations and neglecting gravity, yields the following non-dimensionalized governing system of equations:

$$\nabla \cdot \boldsymbol{V} = 0, \tag{5}$$

$$\frac{\partial^2 u}{\partial x^2} + \xi \nabla_V^2 u + \xi Ra_\omega x \nabla_V^2 T = 0, \tag{6}$$

$$\boldsymbol{V} \cdot \nabla T = \frac{\partial^2 T}{\partial x^2} + \eta \nabla_V^2 T, \tag{7}$$

In Equation (6) the centrifugal Rayleigh number is defined as, $Ra_\omega = \beta_* \Delta T k_{*_x}\ \omega_*^2 L_*^2/(\kappa_{*x}\nu_*)$ and the operator ∇_V is defined as $\nabla_V^2 =$

$\partial^2/\partial y^2 + \partial^2/\partial z^2$ and u is velocity component in the x-direction. As all boundaries are rigid, the solution must follow the impermeability conditions there, i.e. $\boldsymbol{V} \cdot \hat{e}_n = 0$ on the boundaries, where $\hat{e}_n$ is a unit vector normal to the boundary. The temperature boundary conditions are: $T = 0$ at $x = 0$, $T = 1$ at $x = 1$ and $\nabla T \cdot \hat{e}_n = 0$ on all other walls representing the insulation condition on these walls. The partial differential Equations (5–7) forms a non-linear coupled system which together with the corresponding boundary conditions accepts a basic motionless solution of the form: $T_B = x$ and $V_B = 0$.

3. Linear Stability Analysis

We perturb the basic state and the perturbation variables are defined as:

$$[u, T] = [0, T_B] + \left[u', T'\right]. \tag{8}$$

Substituting Equation (8) in Equations (5–7) yields the following equation for the temperature perturbation,

$$\left(\frac{\partial^2}{\partial x^2} + \xi \nabla_V^2\right)\left(\frac{\partial^2}{\partial x^2} + \eta \nabla_V^2\right) T' + \xi\, Ra_\omega x \nabla_V^2 T' = 0, \tag{9}$$

Using normal mode expansions (for the dependant variables) of the form,

$$T' = A e^{i\left(s_y y + s_z z\right)} \theta\,(x)\,, \tag{10}$$

and upon substitution in Equation (9) yields the following ordinary differential equation for θ:

$$\left(\frac{\mathrm{d}^2}{\mathrm{d}x^2} - s^2 \xi\right)\left(\frac{\mathrm{d}^2}{\mathrm{d}x^2} - s^2 \eta\right)\theta - \xi\, Ra_\omega s^2 x \theta = 0. \tag{11}$$

The Galerkin method is adopted to solve Equation (13), so a function of the form $\theta = \sum_{k=1}^{N} a_k \sin(k\pi x)$ which satisfies the boundary conditions $\theta = 0$ at $x = 0$, and $x = 1$ is selected. Substituting in Equation (11) yields,

$$\sum_{k=1}^{N} \left[\left(k^2 + \alpha\right)\left(k^2 + \alpha\varphi\right) - \alpha R x\right] a_k \sin(k\pi x) = 0, \tag{12}$$

where the following scaling variables have been used: $\alpha = \xi s^2/\pi^2$ where $s^2 = s_y^2 + s_z^2$, $R = Ra_\omega/\pi^2$ and $\varphi = \eta/\xi$. Multiplying Equation (12) by orthogonal functions of the form $\sin(l\pi x)$ and integrating over the length of the domain, one obtains a homogenous set of linear algebraic equations of the form

$$\sum_{k=1}^{N}\left\{\left[\frac{1}{2}\left(k^2+\alpha\right)\left(k^2+\alpha\varphi\right)-\frac{1}{4}\alpha R\right]\delta_{lk}+\frac{4kl}{\pi^2\left(l^2-k^2\right)^2}\alpha R\delta_{l+k,2p-1}\right\}a_k=0, \tag{13}$$

for $l=1,2,3,\ldots,M$. In Equation (13) δ_{lk} is the Kronecker delta function and the index p can take arbitrary integer values and stands only for setting the second index in the Kronecker delta function to be an odd integer. Equation (13) has the form $L\left(a_k\right)=0$, representing a homogenous linear system accepting a non-zero solution only for particular values of R such that $\mathbf{det}\left[L\left(a_k\right)\right]=0$. Although the analysis in the current work has been done by solving Equation (13) up to rank $N=8$ for various values of φ, useful information can be drawn by considering the approximation to rank $N=2$. For this rank of approximation the system reduces to two equations that may be presented in the following matrix notation,

$$\begin{bmatrix} \frac{1}{2}(1+\alpha)(1+\alpha\varphi)-\frac{1}{4}\alpha R & \frac{8}{9\pi^2}\alpha R \\ \frac{8}{9\pi^2}\alpha R & \frac{1}{2}(4+\alpha)(4+\alpha\varphi)-\frac{1}{4}\alpha R \end{bmatrix}\begin{bmatrix} a_1 \\ a_2 \end{bmatrix}=0 \tag{14}$$

Taking the determinant of Equation (14) and equating it to zero leads to the characteristic values for R in the form

$$R_c=\frac{1}{\alpha\left(1-\left(\frac{32}{9\pi^2}\right)^2\right)}\left[\left(\lambda_1+\lambda_2\right)\pm\sqrt{\left(\lambda_1-\lambda_2\right)^2+\left(\frac{64}{9\pi^2}\right)^2\lambda_1\lambda_2}\;\right], \tag{15}$$

where $\lambda_1=(1+\alpha)(1+\alpha\varphi)$ and $\lambda_2=(4+\alpha)(4+\alpha\varphi)$. The expression for R_c was evaluated as a function of α for different values of φ at rank $N=2$ and its accuracy was confirmed by evaluating the characteristic values to higher ranks up to $N=8$ by using *Mathematica*™, Wolfram (1991) for numerical calculations. The results for the characteristic Rayleigh number, as a function of the wave number, is shown in Figure 2 for various values of the anisotropy ratio φ. For the case $\varphi=1$ (i.e. $\eta=\xi=1$) we recover the stability results for the case of thermal and permeability isotropy, $Ra_{\omega,cr}=7.81\pi^2$ and $s_{\rm cr}=1.03\pi$, Vadasz (1994). One observes from Figure 2 that for $\varphi<1$ the convection is destabilized, whilst for $\varphi>1$, the convection is stabilized. When $\eta=\xi\neq 1$, the critical Rayleigh number is identical to the isotropic case whilst the critical wave number is reduced by the permeability parameter ξ.

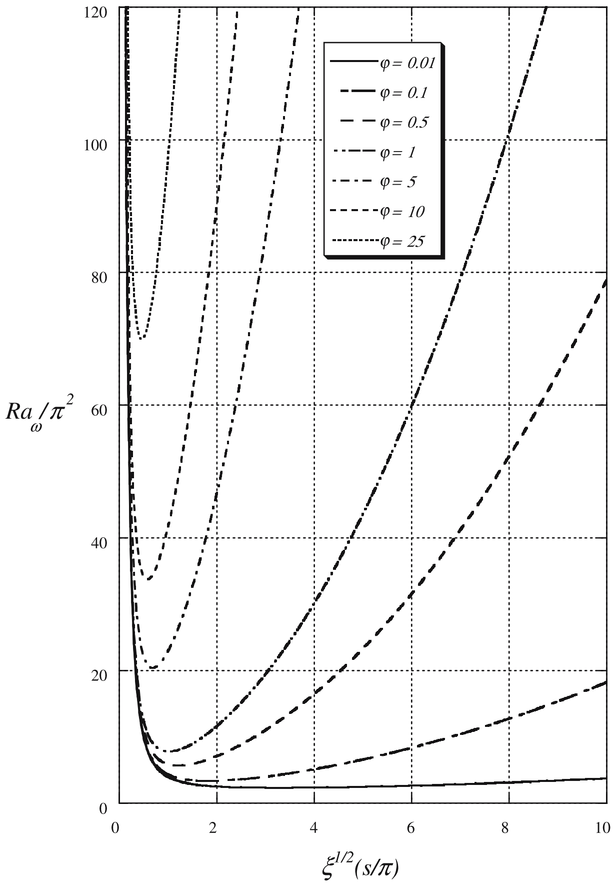

Figure 2. Characteristic Rayleigh number versus wave number for various values of the anisotropy ratio at Rank $N = 2$.

The minima on the curves shown correspond to the critical values for R. These critical values for the Rayleigh number and wave number are shown in Figure 3 as a function of the anisotropy ratio φ. The results show that increasing the anisotropy ratio φ stabilizes the convection. When the thermal anisotropy parameter η is increased in magnitude (for fixed ξ) or the mechanical anisotropy parameter ξ is reduced in magnitude (for fixed η), the net effect is to increase the anisotropy ratio φ thereby stabilizing the convection. Figure 3 also shows that increasing the anisotropy ratio φ (by fixing permeability anisotropy parameter ξ and increasing the thermal anisotropy parameter η) reduces the critical wave number (hence the convection cell size). However, fixing the thermal anisotropy parameter η and reducing the magnitude of the permeability anisotropy parameter ξ results in an increase in the critical wavenumber and destabilizes the convection.

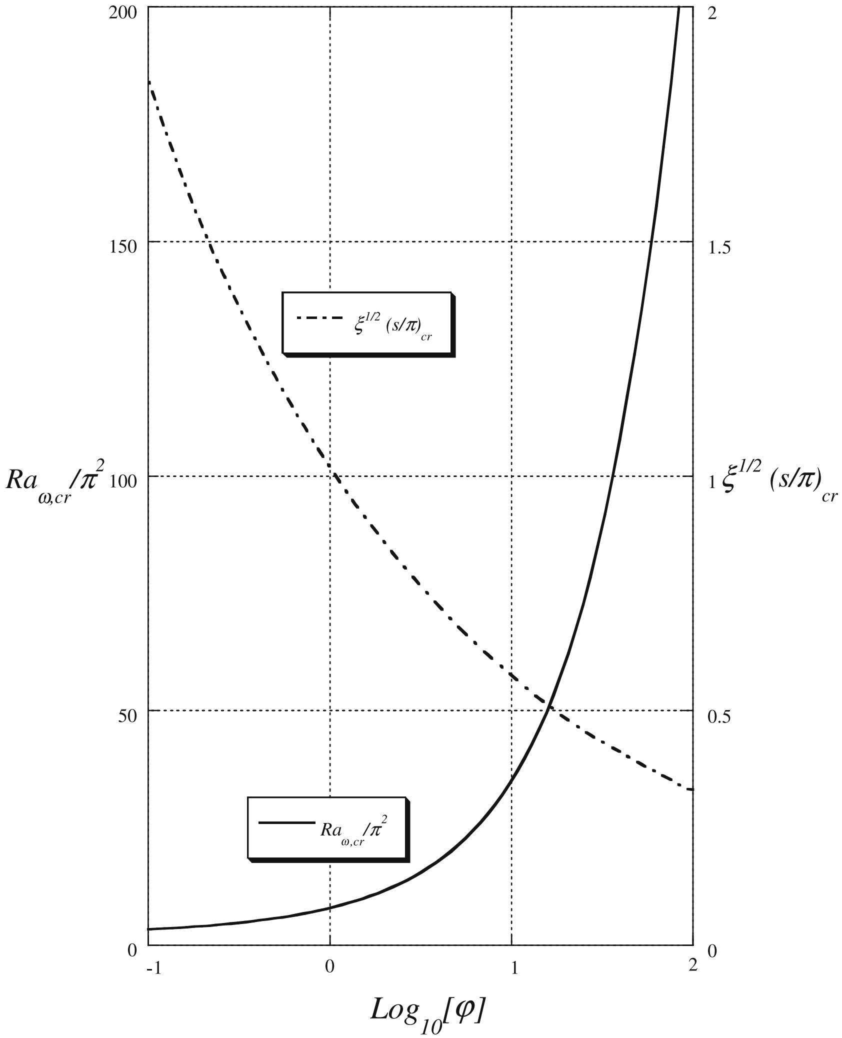

Figure 3. Critical Rayleigh number and wave number versus the anisotropy ratio at Rank $N = 2$.

The stability results obtained by Epherre (1975) in his study concerning anisotropic effects in a porous layer heated from below and subjected to gravitational body forces only (for horizontal isotropy) may be presented in our notation as

$$\left(Ra/\pi^2\right)_{\mathrm{cr}} = \left[1 + \left(\frac{\eta}{\xi}\right)^{1/2}\right]^2 = \left[1 + \varphi^{1/2}\right]^2, \quad \alpha_{\mathrm{cr}} = (\xi\eta)^{-1/2} = \frac{1}{\xi\varphi^{1/2}}, \quad (16)$$

where Ra is the Rayleigh number based on the gravity. Epherre's (1975) stability results clearly show that increasing the anisotropy ratio φ stabilizes the convection (increasing critical Rayleigh number) and reduces the magnitude of the critical wave number (hence the convection cell size). When the thermal anisotropy parameter η is increased in magnitude (for fixed ξ) the convection is stabilized and the critical wave number reduces in magnitude. When the permeability anisotropy parameter ξ is increased in magnitude (for fixed η) the convection is destabilized and the critical wave number reduces in magnitude. The stability results of Epherre (1975) for the porous layer heated from below and subjected to gravity only exhibit similar trends to the stability results for the current study for a rotating porous layer subjected to centrifugal body forces only where the centrifugal body force is in the direction of the temperature gradient.

4. Conclusion

The stability of convection in a horizontal rotating porous layer exhibiting both thermal and mechanical anisotropy is analysed. All of the results are presented as a function of the anisotropy ratio φ. The linear stability theory reveals that increasing the anisotropy ratio φ stabilizes the convection. In general it is also discovered that increasing the thermal anisotropy parameter η (for fixed permeability anisotropy parameter ξ) stabilizes the convection and reduces the convection cell size. However, reducing the permeability anisotropy parameter ξ (for a fixed thermal anisotropy parameter η), destabilizes the convection and increases the magnitude of the critical wave number (and convection cell size).

Acknowledgement

The author would like to thank the National Research Foundation (NRF) for funding this research through the Focus Area Programme-Economic Growth and International Competitiveness: FA2004040700003.

References

Alex, S. M. and Patil, P. R.: 2000, Thermal instability in an anisotropic rotating porous medium, *Heat Mass Transfer* **36**, 159–163.

Amberg, G. and Homsy, G. M.: 1993, Nonlinear analysis of buoyant convection in binary solidification to channel formation, *J. Fluid Mech.* **252**, 79–98.

Anderson, D. M. and Worster, M. G.: 1995, Weakly non-linear analysis of convection in mushy layers during the solidification of binary alloys, *J. Fluid Mech.* **302**, 307–331.

Epherre, J. F.: 1975, Critere d' apparition de la convection naturelle dans une couche poreuse anisotrope, *Rev. Gen. Thermique* **168**, 949–950.

Govender, S.: 2003, On the linear stability of large Stefan number convection in rotating mushy layers for a new Darcy equation formulation, *Transp. Porous Media* **51**(2), 173–189.

Govender, S. and Vadasz, P.: 2002, Weak nonlinear analysis of moderate Stefan number oscillatory convection in rotating mushy layers, *Transp. Porous Media* **48**(3), 353–372.

McKibbin, R.: 1986, Thermal convection in a porous layer: effects of anisotropy and surface boundary conditions, *Transp. Porous Media* **1**, 271–292.

Patil, P. R., Parvathy, C. P. and Venkatakrishnan, K. S.: 1989, Thermohaline instability in a rotating anisotropic porous medium, *Appl. Sci. Res.* **46**, 73–88.

Sample, A. K. and Hellawell, A.: 1984, The mechanisms of formation and prevention of channel segregation during alloy solidification, *Metall. Trans. A* **15**A, 2163–2173.

Sarazin, J. R. and Hellawell, A.: 1998, Channel formation in Pb–Sb, and Pb–Sn–Sb alloy ingots and comparison with the system $NH_4Cl - H_2O$, *Metall. Trans. A* **19**A, 1861–1871.

Storesletten, L.: 1993, Natural convection in a horizontal porous layer with anisotropic thermal diffusivity, *Transp. Porous Media* **12**, 19–29.

Vadasz, P.: 1994, Stability of free convection in a narrow porous layer subjected to rotation, *Int. Commun. Heat Mass Transfer* **21**(6), 881–890.

Vaidyanathan G., Sekar R. and Ramanathan A.: 1998, Effects of rotation and anisotropy of a porous medium on ferroconvection, *Indian J. Eng. Mater. Sci.* **5**, 436–440.

Wolfram, S.: 1991, *Mathematica TM: A System for Doing Mathematics by Computer*, 2nd edn., Wolfram Research, Addison-Wesley, Redwood City, CA.

Worster, M. G.: 1992, Instabilities of the liquid and mushy regions during solidification of alloys, *J. Fluid. Mech.* **237**, 649–669.